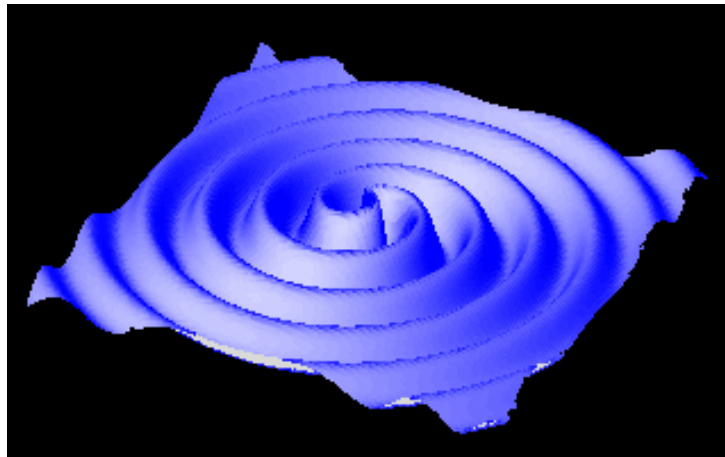


**Astrophysical sources of gravitational waves:
from core-collapse of massive stars to double compact object binaries**

L. Zampieri

INAF-Osservatorio Astronomico di Padova

Lecture for the Heraeus School 2015, Padova



**Astrophysical sources of gravitational waves:
from core-collapse of massive stars to double compact object binaries**

OUTLINE

1. INTRODUCTION
2. GRAVITATIONAL RADIATION
3. GRAVITATIONAL WAVES IN THE AFTERMATH OF A SUPERNOVA
4. DOUBLE PULSARS AND GRAVITATIONAL RADIATION FROM INSPIRAL AND MERGER OF DOUBLE COMPACT OBJECT BINARIES

*Figures in this slides are taken from *Wikipedia* (<http://wikipedia.org>) or other on-line resources (as referenced in the caption of each figure or in the highlighted link).

**Astrophysical sources of gravitational waves:
from core-collapse of massive stars to double compact object binaries**

1. INTRODUCTION

- (a) **Electromagnetic and gravitational radiation: Analogies and differences**
- (b) **Some basic concepts: Waveforms, wave polarizations, laser interferometer gravitational wave detectors**
- (c) **Gravitational wave strength: Quadrupole formula and order of magnitude estimates**
- (d) **Sensitivity plots and rate estimates**

**Astrophysical sources of gravitational waves:
from core-collapse of massive stars to double compact object binaries**

Electromagnetic and gravitational radiation: Analogies and differences

- **Analogies** between electromagnetic waves (EWs) and gravitational waves (GWs):
 - In vacuum (in the weak gravity limit) they both obey a wave equation ...

$$\nabla^2 A - \frac{1}{c^2} \frac{\partial^2 A}{\partial t^2} = 0 \quad (1)$$

- ... and propagate at the speed of light c
 - They have polarization states: linear/circular for EWs, +/x for GWs
- ... and **differences**:
 - EWs propagate through space-time, while GWs are oscillations of the space-time itself
 - Astronomical EWs are most often incoherent superposition of emissions from single particles, while GWs are produced by coherent bulk motions of huge amounts of mass-energy

- EWs form images of their sources, GWs do not (they carry a 'stereophonic' description of their sources)
- EWs interact easily with matter, while GWs travel nearly unscattered
- The frequency range of astronomical EWs and GWs are very different

Analogies make GWs more easily understandable, differences will teach us something new as:

- Details of the bulk motion of dense concentration of mass-energy in unprobed space-times (unaccessible through EWs)
- New 'surprises' (as always when a new window is opened on the Universe)

**Astrophysical sources of gravitational waves:
from core-collapse of massive stars to double compact object binaries**

Some basic concepts

Waveforms

According to General Relativity (GR) GWs can be described as ripples in space-time propagating at the speed of light c . When a GW reaches a freely moving object, it will feel the wave ripples.

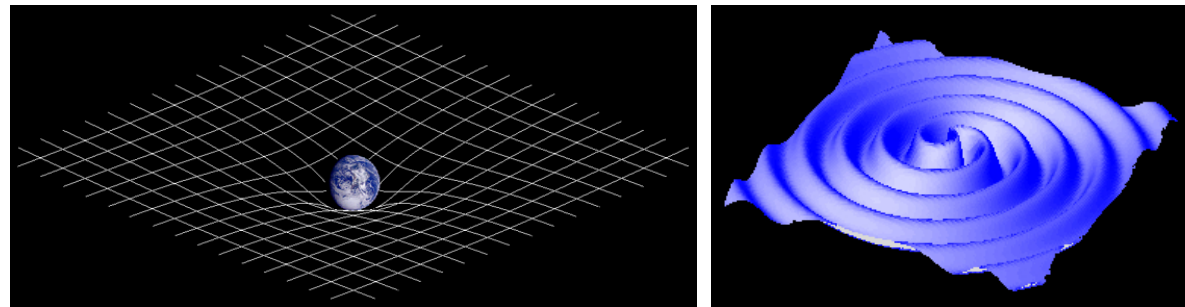


Figure 1 – Left: Representation of the curved space-time around a massive body. Right: Representation of a GW as ripples in space-time propagating from a source at the center.

Let's assume that the quantity h is some measure of the strength of a GW. Its time evolution $h(t)$ is often called a **waveform**. $h(t)$ is determined solving the Einstein field equations of GR.

Polarization

A GW has **2 polarizations** (oscillations modes), denoted with '+' and 'x'.



Figure 2 – Left: Snapshot of a + polarization GW.
Right: Snapshot of a x polarization GW.

The corresponding waveforms are $h_+(t)$ and $h_x(t)$.

Laser interferometer GW detector

A laser interferometer GW detector (GW interferometer) consists of 4 test masses, hanging from vibration-isolated supports, and an optical system (based on laser light reflection) for measuring distances between masses (through phase interferometry).

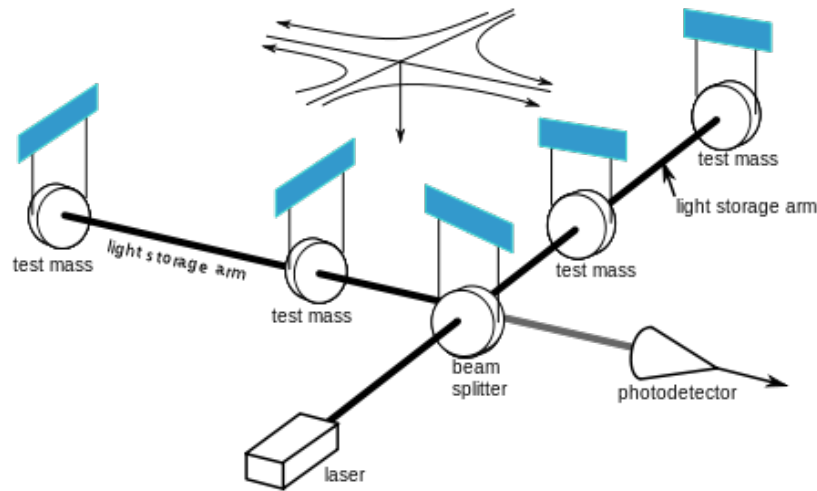


Figure 3 – Left: Schematic view of a GW interferometer (credit: Malyszczk). Right: Laser Interferometer GW Observatory (LIGO) Hanford installation. Each arm extends for 4 km (credit: Caltech).

When a GW (with oscillation frequency $\gg 1$ Hz mass-pendulum frequency) passes through the detector, it will move the masses back and forth, modifying their relative position (they are essentially free to move in the horizontal direction). If L_1 and L_2 are the distances of the masses along the two arms, in general the change ΔL (measured by the laser optical system) is:

$$\frac{\Delta L(t)}{L_{1,2}} = a_+ h_+(t) + a_x h_x(t) = h(t) \quad \text{GW strain} \quad (2)$$

where a_+ and a_x depend on the direction of the source and the orientation of the GW inteferometer.

**Astrophysical sources of gravitational waves:
from core-collapse of massive stars to double compact object binaries**

GW strength

A GW is produced by coherent bulk motions of huge amounts of mass. Similarly to the well known fact that accelerating charges produce EWs, in quite general terms accelerating masses can produce GWs.

Quadrupole formula

From GR, a first estimate of the strength of a GW can be obtained from the so called **quadrupole formula**, that links it to the second time derivative of a particular mass distribution, its quadrupole moment Q (with the dimensions of a moment of inertia):

$$h \simeq \frac{G}{c^4} \frac{\ddot{Q}}{r} \quad (3)$$

where r is the source distance. More specifically, h does not depend on the time-variation of a spherical or (equal-aspect-ratio) axysimmeytric mass distribution, but on higher-order time-dependent deformations.

The strongest sources are highly non-spherical and hence have $Q \simeq MR^2$, where M is their mass and R their size. If R varies on a characteristic time Δt , then:

$$h \simeq \frac{G}{c^4} \frac{M(R/\Delta t)^2}{r} = \frac{GM}{c^2 r} \frac{v^2}{c^2} = \frac{2G}{c^2} \frac{E_{kin}^{ns}/c^2}{r} \quad (4)$$

where v and E_{kin}^{ns} refer to the non-spherical motion.

Order of magnitude estimates

A huge amount of gravitationally-induced E_{kin}^{ns} requires a huge amount of gravitational potential energy. This implies in turn that the source is very compact. Colliding compact objects are among the strongest sources of GWs.

For neutrons stars (NSs) and stellar-mass black holes (BHs) with $E_{kin}^{ns}/c^2 \sim 1M_{\odot}$:

$$h \simeq \frac{2G}{c^2} \frac{E_{kin}^{ns}/c^2}{r} = 10^{-21} (r/200 \text{ Mpc}) \quad (5)$$

Considering the present measurement accuracy of ΔL through laser interferometers ($\simeq 10^{-16}$ cm, or 1/1000 the diameter of an atomic nucleus), this sets the scale of ground-based GW inteferometers:

$$L = \Delta L/h \simeq 1 \text{ km} \quad (6)$$

Astrophysical sources of gravitational waves: from core-collapse of massive stars to double compact object binaries

Sensitivity plots and rate estimates

The sensitivity to GW detection is usually represented as a function of GW frequency f , that depends on the characteristic size and dynamical time-scale of the source. For NSs and stellar-mass BHs: $f \sim R/0.1c = 10^3$ Hz.

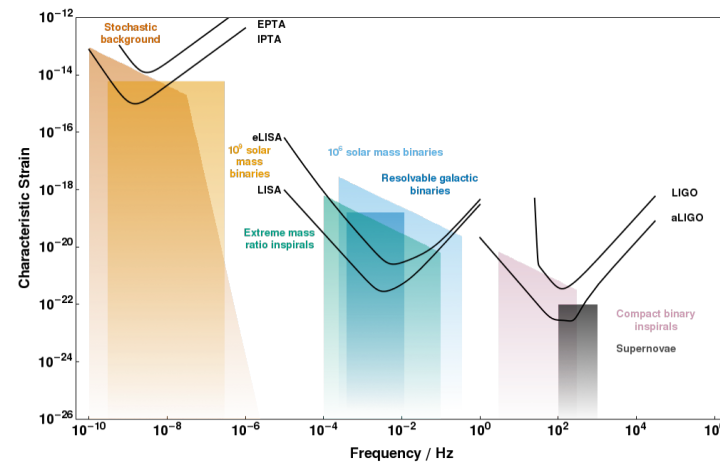


Figure 4 – Noise curves for a selection of detectors and the characteristic GW strain of potential astrophysical sources (credit: Christopher Moore, Robert Cole and Christopher Berry).

The sensitivity is limited at low frequencies by seismic noise and at high frequency by laser photon Poissonian noise.

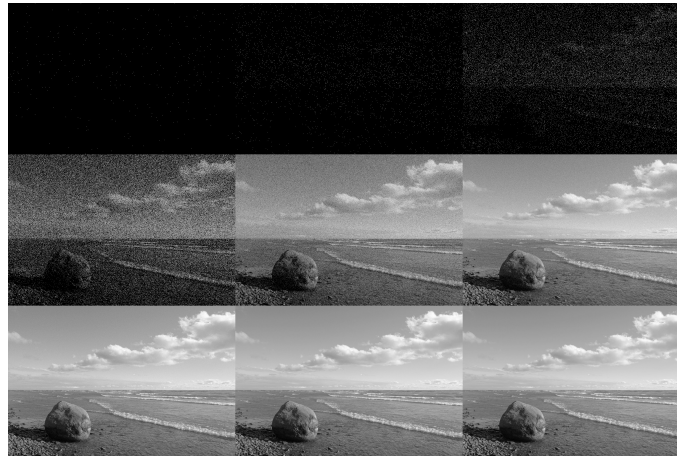


Figure 5 – Photon noise simulation. Number of photons per pixel increases from left to right and from upper row to bottom row (credit: Mdf).

How many events to expect per year? Clearly, it depends on the type of event.

For colliding NS-NS binaries:

- We know some of these binaries in our own Galaxy that will merge in less than a Hubble time (e.g. PSR 1913+16, PSR J0737-3039). From the inferred local density of these systems (and taking into account pulsar survey selection

effects), in the most favorable case there could be $\sim 10 - 100$ events per year up to ~ 200 Mpc.

- A fraction of Gamma-ray Bursts (short GRBs, with duration < 2 s) are believed to be associated to NS-NS or BH-NS mergers. From the observed rate and correcting for the fact that we probably see only the EW emission of sources beamed towards us, the estimated rate is 0.1-10 events per year up to ~ 200 Mpc.
- Theoretical estimates are also derived from detailed calculations of binary evolution in isolation and in star clusters (see M. Mapelli's lecture).

**Astrophysical sources of gravitational waves:
from core-collapse of massive stars to double compact object binaries**

2. GRAVITATIONAL RADIATION

- (a) **General Relativity in a nutshell**
- (b) **GWs in the weak gravity limit**
- (c) **Generation of GWs: The mass quadrupole equation**
- (d) **Generation of GWs: Energy loss**
- (e) **Non-linear description of GWs: Perturbation theory, post-Newtonian theory, numerical Relativity**

**Astrophysical sources of gravitational waves:
from core-collapse of massive stars to double compact object binaries**

General Relativity in a nutshell

GR describes gravity as geometry. A crucial notion of geometry is distance which, in a Euclidian space, does not change as we vary coordinate system.

Similarly, in GR 4-dimensional space-time the squared (proper) distance between events at coordinates x^α and $x^\alpha + dx^\alpha$ does not vary with coordinates and is written as:

$$ds^2 = g_{\alpha\beta} dx^\alpha dx^\beta \quad \alpha, \beta = 0, \dots, 3 \quad x^0 = ct \quad (7)$$

where repeated indices (in superscript and subscript positions) are summed together.

If we know the geometry of space-time, described by the so called **metric** $g_{\alpha\beta}$, we can compute ds^2 .

Consider now a trajectory ζ^α describing an observer in space-time. Along it, the **(proper) time** τ , measured by the observer himself, will vary. Integrating eq. (7) along the trajectory ζ^α from event A to B, we obtain:

$$s = \int_A^B ds = \int_A^B \sqrt{g_{\alpha\beta} dx^\alpha dx^\beta} = \int_A^B d\tau \sqrt{g_{\alpha\beta} u^\alpha u^\beta} \quad (8)$$

$$u^\alpha = \frac{dx^\alpha}{d\tau} \quad 4 - \text{velocity of the observer} \quad (9)$$

The 4-velocity of the observer that follows the shortest path between event A and B is obtained extremizing s and obeys to the following **geodesic equation**:

$$\frac{du^\alpha}{d\tau} + \Gamma_{\beta\gamma}^\alpha u^\beta u^\gamma = 0 \quad (10)$$

$$\Gamma_{\beta\gamma}^\alpha = \frac{1}{2} g^{\alpha\mu} (\partial_\gamma g^{\mu\beta} + \partial_\beta g^{\gamma\mu} - \partial_\mu g^{\beta\gamma}) \quad \text{connection} \quad (11)$$

where $g^{\alpha\beta} = g^{\alpha\mu} g^{\beta\nu} g_{\mu\nu}$ (operation of rising indices) and $\partial_\alpha = \partial/\partial x^\alpha$.

By assumption, the shortest path in space-time determined by the geodesic equation is exactly the path followed by a freely moving object, subject only to the action of **gravity**. The connection determines the free motion of such an object in space-time, specifying how curve it is.

Other quantities introduced to measure the space-time curvature are:

$$R_{\beta\gamma\delta}^{\alpha} = \partial_{\gamma}\Gamma_{\beta\delta}^{\alpha} - \partial_{\delta}\Gamma_{\beta\gamma}^{\alpha} + \Gamma_{\mu\gamma}^{\alpha}\Gamma_{\beta\delta}^{\mu} - \Gamma_{\mu\delta}^{\alpha}\Gamma_{\beta\gamma}^{\mu} \quad \text{Riemann curvature} \quad (12)$$

$$R_{\alpha\beta} = R_{\alpha\mu\beta}^{\mu} \quad \text{Ricci curvature} \quad (13)$$

$$R = R_{\mu}^{\mu} \quad \text{Ricci scalar} \quad (14)$$

$$G_{\alpha\beta} = R_{\alpha\beta} - \frac{1}{2}g_{\alpha\beta}R \quad \text{Einstein curvature} \quad (15)$$

Besides dealing with the mathematics of the curved space-time, GR describes also how matter and energy evolve in it and interact with it. The quantity that contains information on matter and energy is the [stress-energy tensor](#), whose components are assumed to have the following physical meaning:

$$T^{00} \equiv \text{Local mass - energy density} \quad (16)$$

$$T^{0j} \equiv \text{Local mass - energy flux } (\times c) \quad (17)$$

$$T^{ij} \equiv \text{Local momentum flux or pressure } (\times c^2) \quad i, j = 1, \dots, 3 \quad (18)$$

Local conservation of energy and momentum is expressed by:

$$\partial_{\alpha}T^{\beta\gamma} + T^{\beta\mu}\Gamma_{\alpha\mu}^{\gamma} + T^{\mu\gamma}\Gamma_{\alpha\mu}^{\beta} = 0 \quad (19)$$

Einstein proposed that the stress-energy tensor of matter-energy is the source of space-time curvature:

$$G_{\alpha\beta} = \frac{8\pi G}{c^4} T^{\alpha\beta} \quad \text{Einstein equation} \quad (20)$$

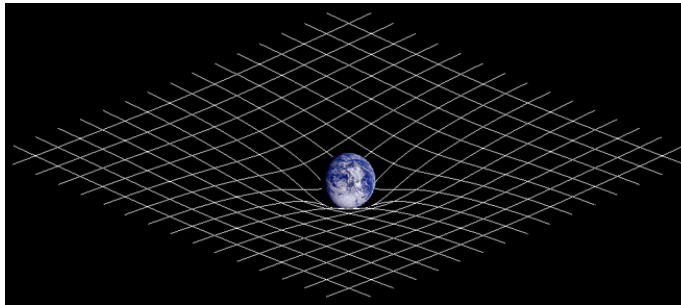


Figure 6 – Representation of the curved space-time around a massive body.

**Astrophysical sources of gravitational waves:
from core-collapse of massive stars to double compact object binaries**

GWs in the weak gravity limit

We now assume to be in the weak gravity limit, in which the space-time geometry is very close to that of Special Relativity:

$$g_{\alpha\beta} = \eta_{\alpha\beta} + h_{\alpha\beta} \quad |h_{\alpha\beta}| \ll 1 \quad (21)$$

$$\eta_{\alpha\beta} = \text{diag}(-1, 1, 1, 1) \quad (22)$$

Using eq. (22) and retaining only term to first order in the metric perturbation $h_{\alpha\beta}$, the Einstein curvature (eq. [15]) becomes:

$$G_{\alpha\beta} = \frac{1}{2}(\partial_\alpha \partial^\mu h_{\mu\beta} + \partial_\beta \partial^\mu h_{\mu\alpha} - \partial_\alpha \partial_\beta h - \square h_{\alpha\beta} + \eta_{\alpha\beta} \square h - \eta_{\alpha\beta} \partial^\mu \partial^\nu h_{\mu\nu}) \quad (23)$$

$$h = \eta^{\alpha\beta} h_{\alpha\beta} \quad \square = \eta^{\alpha\beta} \partial_\alpha \partial_\beta \quad (24)$$

that can be simplified in:

$$G_{\alpha\beta} = \frac{1}{2}(\partial_\alpha \partial^\mu \bar{h}_{\mu\beta} + \partial_\beta \partial^\mu \bar{h}_{\mu\alpha} - \square \bar{h}_{\alpha\beta} - \eta_{\alpha\beta} \partial^\mu \partial^\nu \bar{h}_{\mu\nu}) \quad (25)$$

$$\bar{h}_{\alpha\beta} = h_{\alpha\beta} - \frac{1}{2} \eta_{\alpha\beta} h \quad \bar{h} = -h \quad (26)$$

A further major simplification occurs performing the change of coordinates $x^\alpha \rightarrow x^\alpha + \xi^\alpha$ (the Riemann curvature remains unchanged) and imposing that, in the new coordinates, $\partial^\mu \bar{h}_{\mu\nu} = 0$ (Lorentz gauge):

$$G_{\alpha\beta} = -\frac{1}{2}\square\bar{h}_{\alpha\beta} \quad (27)$$

Then, the Einstein equation(s) in weak gravity becomes:

$$\square\bar{h}_{\alpha\beta} = -\frac{16\pi G}{c^4}T_{\alpha\beta} \quad (28)$$

This is a [wave equation](#) (similar to that for the EWs obtained from the Maxwell equations) and has the formal solution:

$$\bar{h}_{\alpha\beta}(t) = \frac{4G}{c^4} \int \frac{T_{\alpha\beta}(t - r/c)}{r} dV \quad (29)$$

where r is the source distance (assumed much larger than the source size).

**Astrophysical sources of gravitational waves:
from core-collapse of massive stars to double compact object binaries**

Generation of GWs: The mass quadrupole equation

In weak gravity, to first order in $h_{\alpha\beta}$ the local conservation of energy and momentum (eq. [19]) simplifies to:

$$\partial^\alpha T_{\alpha\beta} = 0 \quad \partial^0 T_{00} + \partial^j T_{j0} = 0 \quad \partial^0 T_{0j} + \partial^i T_{ij} = 0 \quad i, j = 1, \dots, 3 \quad (30)$$

Using these expressions, integrating by parts, converting volume integrals to surface integrals, and taking the surfaces at large distance from the source, one has:

$$\int T_{ij} dV = \frac{1}{2} \int x_i x_j \partial^k \partial^l T_{kl} dV = \frac{1}{2} \int x^i x^j \partial^t \partial^t T_{00} dV = \frac{1}{2} \frac{d^2}{dt^2} I_{ij} \quad (31)$$

$$I_{ij} = \int x^i x^j T_{00} dV \quad \text{quadrupole moment} \quad (32)$$

Assuming very distant sources ($r \simeq \text{const}$), from eqs. (29) and (31) we finally obtain:

$$\bar{h}_{ij} = \frac{2G}{rc^4} \frac{d^2}{dt^2} I_{ij} \quad (33)$$

$$I_{ij} = \int x^i x^j T_{00} dV \quad \text{quadrupole moment} \quad (34)$$

A last technical detail concerns the fact that only spatial components transverse to the direction of propagation \vec{n} of the wave represent really (gauge-independent) radiative solutions (GWs). To account for this, eq. (33) is projected orthogonal to \vec{n} using the (trace-free) projector $P_{ki}P_{lj} - (1/2)P_{kl}P_{ij}$ (where $P_{ij} = \delta_{ij} - n_in_j$), giving the transverse **mass quadrupole equation**:

$$h_{ij}^{TT} = \bar{h}_{kl}(P_{ki}P_{lj} - \frac{1}{2}P_{kl}P_{ij}) \quad (35)$$

$$h_{ij}^{TT} = \frac{2G}{rc^4} \frac{d^2}{dt^2} \tilde{I}_{kl}(P_{ki}P_{lj} - \frac{1}{2}P_{kl}P_{ij}) \quad (36)$$

$$\tilde{I}_{ij} = I_{ij} - \frac{1}{3}\delta_{ij}I \quad \text{reduced quadrupole moment } (I = I_{ii}) \quad (37)$$

The reduced quadrupole is more convenient to use and it is possible to show that the term $(1/3)\delta_{ij}I$ does not contribute to eq. (36).

**Astrophysical sources of gravitational waves:
from core-collapse of massive stars to double compact object binaries**

Generation of GWs: Energy loss

GWs transport energy and momentum. The emitted energy depends on the square of the wave amplitude. Similarly, to compute the energy loss from GWs requires a treatment to second order in the strain amplitude, even in weak gravity (perturbation theory).

The result of this calculation for the projection of the $0k$ component of the GW stress-energy tensor along the wave direction \vec{n} (representing the GW radial energy flux) is:

$$\frac{\partial^2 E^{GW}}{\partial A \partial t} \equiv T_{tk}^{GW} n^k = \frac{c^4}{32\pi G} \langle \partial_t h_{ij}^{TT} \partial_r h_{ij}^{TT} \rangle \quad (38)$$

where $\langle \rangle$ denotes average over long scales (larger than the GW wavelength)

Using eq. (36), keeping in mind that \tilde{I}_{kl} is evaluated at the retarded time $(t - r/c)$ and integrating over surface ($dA = r^2 \sin \theta d\theta d\phi$), one obtains the GW luminosity:

$$L^{GW} \equiv \int T_{0k}^{GW} n^k dA = \frac{1}{5} \frac{G}{c^5} \langle \frac{d^3 \tilde{I}_{ij}}{dt^3} \frac{d^3 \tilde{I}_{ij}}{dt^3} \rangle \quad (39)$$

**Astrophysical sources of gravitational waves:
from core-collapse of massive stars to double compact object binaries**

**Non-linear description of GWs:
Perturbation theory, post-Newtonian theory, numerical Relativity**

If the GW propagates in a non-flat space-time, the calculation becomes more complex. Different approximate approaches can be adopted, such as perturbation theory or post-Newtonian theory. They are both based on the idea to expand the Einstein equations using some suitably small parameter.

Perturbation theory

The space-time is exact, e.g. that of a **Schwarzschild BH of mass M** :

$$ds^2 = g_{\alpha\beta}^{BH} dx^\alpha dx^\beta = - \left(1 - \frac{r_S}{r}\right) c^2 dt^2 + \left(1 - \frac{r_S}{r}\right)^{-1} r^2 d\Omega^2 \quad (40)$$

$$r_s = 2GM/c^2 \quad \text{Schwarzschild radius} \quad (41)$$

where we adopted Schwarzschild spherical coordinates ($d\Omega^2 = d\theta^2 + \sin^2\theta d\phi^2$). However, the GW is again described as a small perturbation $h_{\alpha\beta}$, so that:

$$g_{\alpha\beta} = g_{\alpha\beta}^{BH} + h_{\alpha\beta} \quad (42)$$

If the perturbation is caused by a small body of mass m orbiting the BH, the expansion parameter in the Einstein equations is taken to be the mass ratio m/M . This approach is then an *ideal tool for extreme mass ratio captures*, where a neutron star or stellar-mass BH is dynamically injected into a strong-field orbit of a massive or supermassive BH.

Post-Newtonian theory

In the case of two orbiting NSs or BHs of nearly equal masses, the mass ratio is not a good expansion parameter. One can try with a different approach, starting from writing the metric in **harmonic or de Donder coordinates**:

$$g^{\alpha\beta} = \frac{1}{\sqrt{-g}}(\eta^{\alpha\beta} + h^{\alpha\beta}) \quad (43)$$

$$h^{\alpha\beta} \equiv \sqrt{-g}g^{\alpha\beta} - \eta^{\alpha\beta} \quad (44)$$

where g is the determinant of $g_{\alpha\beta}$. This looks similar to the flat space-time perturbation, but $h^{\alpha\beta}$ is not necessarily small.

Using the metric (43), the Einstein equations can be expanded in terms of the potential $\phi = GM/rc^2$ (post-Newtonian expansion).

Numerical Relativity

The direct method to solve Einstein equations in a generic metric is to integrate them numerically. However, they have first to be cast in such a way that they can

be solved as a function of time starting from an initial state, as for the Maxwell equations (evolutionary/hyperbolic system of partial differential equations).

There are different mathematical formulations of the Einstein evolution equations, such as the ADM equations (Arnowitt, Deser & Misner 1962) or the BSSN equations (Baumgarte & Shapiro 1999; Shibata & Nakamura 1995).

**Astrophysical sources of gravitational waves:
from core-collapse of massive stars to double compact object binaries**

3. GRAVITATIONAL WAVES IN THE AFTERMATH OF A SUPERNOVA

- (a) **Core-collapse (CC) of massive stars and supernova explosion: Late stages and collapse**
- (b) **CC of massive stars and supernova explosion: Dynamics and neutrino driven wind**
- (c) **GWs from non-spherical CC**
- (d) **Core bounce, oscillations, convection and radiation-hydro instabilities: Properties of the GW signal**
- (e) **Rotation-induced bar instability of the newborn neutron star**

**Astrophysical sources of gravitational waves:
from core-collapse of massive stars to double compact object binaries**

CC of massive stars and supernova explosion: Late stages and collapse

Masses of bound nuclei (m_b) are smaller than the sum of the masses of free individual nucleons (m_n). $\Delta m = m_n - m_b$ is a measure of the **nuclear binding energy**:

$$E_b = \Delta mc^2 \quad (45)$$

In stars nucleons are assembled in different nuclear configurations, releasing binding energy E_b that maintains hydrostatic equilibrium.

This goes over for millions or billions of years. Depending on the mass M_* of the star, different nuclear reaction histories occur:

- $M_* < 8M_\odot$: After igniting H into He and, possibly, He into C and O in their nuclei, these stars end their lives as **Helium or Carbon-Oxygen white dwarfs**, supported by pressure of degenerate electrons
- $M_* > 8M_\odot$: These stars achieve sufficiently high temperatures ($6 \times 10^8 - 10^9$ K) to ignite C and further burning stages (O, Ne, Mg, Si) in their cores, up to the formation of ^{56}Fe , which is the most tightly bound nucleus.

But, **at a certain point, some stars explode catastrophically.**

The sudden appearance of these explosions in the sky (called *new stars*) is recorded in the most ancient documents (especially in China). The modern history of these events began in 1885 with the discovery of bright *new stars* in the Andromeda galaxy and other *spiral nebulae*.

Their enormous luminosity was definitely established after the extragalactic nebulae were placed at their actual distances, leading Baade & Zwicky (1934) to define them as **super-novae**.



Figure 7 – From left to right: supenovae 199em, 1998bu, 1994D (credit: N. B. Suntzeff).

These explosions involve enormous amounts of (radiated and kinetic) energy:

$$\begin{aligned} L &\sim 3 \times 10^{42} \text{ erg/s} & \text{for } t &\sim 100 \text{ days} = 8 \times 10^6 \text{ s} & \rightarrow & E_r \sim L \times t = 10^{49} \text{ erg} \\ M &\sim 5 - 10 M_{\odot} & \text{at } v &\sim 3 \times 10^8 \text{ cm/s} & \rightarrow & E_k \sim Mv^2 = 10^{51} \text{ erg} \end{aligned}$$

What makes a star to explode as a supernova?

Going back to the evolution of stars with $M_* > 8M_\odot$, we left them with a core comprised of ^{56}Fe .

The **following catastrophic chain of events** occurs at this point:

- The core is supported by electron degeneracy pressure, because no further exo-energetic nuclear reactions occur (^{56}Fe is the most tightly bound nucleus).
- *Si is continuing to burn in a shell around the core, hence continually increasing its mass.*
- When the core exceeds $\sim 1.4M_\odot$, it has no other energy source to support the pressure. It becomes unstable and starts to contract.

The core and the star are doomed. *In a fraction of a second:*

- a temperature (entropy) increases and heavy nuclei are photo-disintegrated into free nucleons
- b electrons are captured onto nuclei and their contribution to the pressure is removed
- c temperature increases further and the remaining electrons become relativistic, softening the equation of state (further reducing the internal pressure)

The contraction of the core turns into a collapse

**Astrophysical sources of gravitational waves:
from core-collapse of massive stars to double compact object binaries**

CC of massive stars and supernova explosion: Dynamics and neutrino driven wind

The collapse is so fast and the core is so dense that all released **gravitational binding energy** $E_{b,g}$ remains trapped in it:

$$\begin{aligned} M_{core} &\sim 1 M_{\odot} & R_{core} &\sim 10 \text{ km} \\ E_{b,g} &\sim GM_{core}c^2/R_{core} && \sim 10^{53} \text{ erg} \end{aligned} \quad (46)$$

During collapse, neutrinos are copiously produced by electron capture onto nuclei ($p + e^- \rightarrow n + \nu_e^-$) and other processes, and play a leading role in the **explosion dynamics**, as shown by detailed numerical radiation-hydrodynamics calculations. This leads also to an increasing neutronization of the core.

- When the density ρ is of the order of 10^{12} g/cm^3 , neutrinos start to have significant interactions with matter. *They do not freely escape but diffuse outwards* ($\tau_{\nu} > 1$).
- Their diffusion lengthscale and timescale are: $\lambda_{\nu} \sim 10 \text{ cm} \ll R_{core}$, $t_{\nu} = 1 - 10 \text{ s}$. t_{ν} is larger than the dynamical time, so that neutrinos are trapped (advected inward)

- **When the inner core ($\sim 0.5 - 0.8M_{\odot}$) reaches nuclear densities ($\rho \sim 10^{14}$ g/cm³), the equation of state suddenly stiffens (nuclear matter EOS).** Short-range nuclear force is repulsive at very small distances.
- The inner core halts and the outer core bounces, driving a shock wave through the infalling matter. This prompt shock propagates outwards, but loses energy by dissociating Fe in the outer core.
- When the prompt shock reaches the neutrino sphere (where $\tau_{\nu} = 1$), additional e-captures on free protons remove energy from the shock, giving rise to a strong burst of electron neutrinos (prompt neutrino burst). **A significant fraction of the core gravitational binding energy $E_{b,g}$ is carried away at this stage ($\sim 10 - 20$ ms after CC).**
- **The shock then loses energy and pressure support, and stalls** at a radius of $\sim 100 - 200$ km.
- **At ~ 1 s after CC** the bulk of neutrinos diffuse outwards carrying away the remaining fraction of $E_{b,g}$. The core becomes a **newly born neutron star**.
- Energy deposition via neutrino absorption ($n + \nu_e \rightarrow p + e^{-}$) below the shock boosts pressure and 'rejuvenates' the shock, causing the **supernova explosion** (delayed shock). Only $0.01E_{b,g} = 10^{51}$ erg is deposited (of the order of the observed ejecta kinetic energy), but sufficient to initiate a powerful explosion.

- **Strong neutrino heating drives a flow of protons and neutrons, inducing convective overturn from above the proto-NS** (neutrino-driven wind).
- In 3D simulations, hydrodynamical instabilities are seen to develop at this stage: **convection in the neutrino-driven wind** increases efficiency of neutrino heating behind the shock and another large-scale instability, the **standing accretion-shock instability (SASI)**, has a similar beneficial effect.

SN 1987A exploded on February 23, 1987 in the Large Magellanic Cloud. It is the **nearest and brightest supernova** after that recorded in our Galaxy by Kepler in 1604. It was observed in every band of the electromagnetic spectrum and the **first to be detected through its initial burst of neutrinos (few hours before)**.

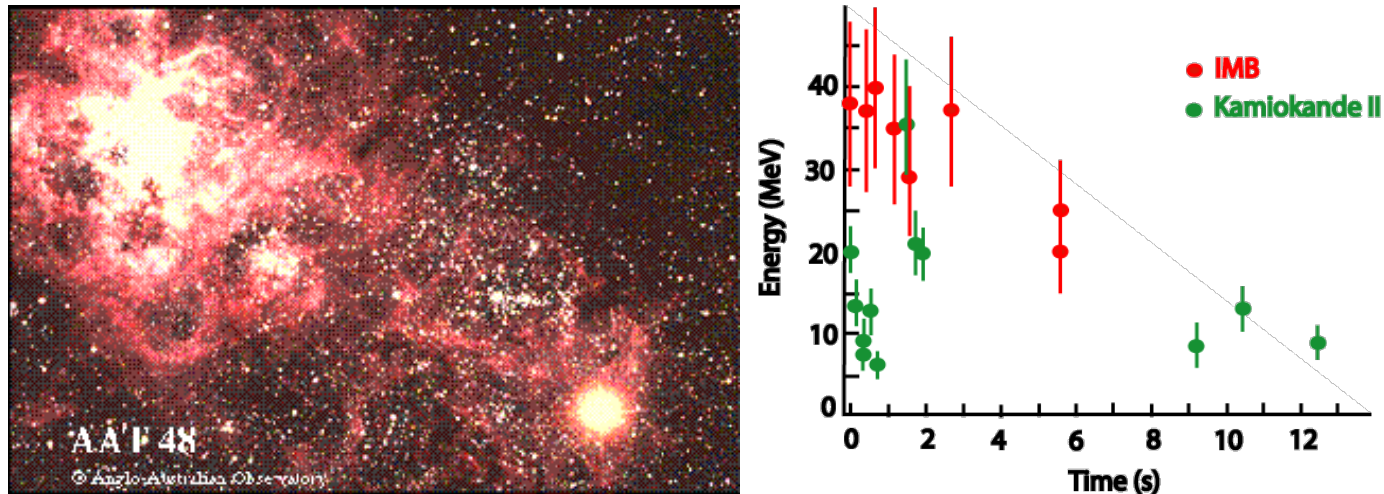


Figure 8 – Left: SN 1987A. Right: Neutrinos from SN 1987A (court. of D. McCray).

**Astrophysical sources of gravitational waves:
from core-collapse of massive stars to double compact object binaries**

GWs from non-spherical CC

The collapse and core's subsequent evolution could be a significant source of GWs (involving coherent bulk motions of huge amounts of mass). Emitted GWs are unimportant for the collapse dynamics.

However, as discussed above, GW emission cannot be produced, to leading order, by the time-variation of a spherical or (equal-aspect-ratio) axisymmetric mass distribution. Thus, a spherical or (equal-aspect-ratio) axisymmetric collapsing core would not emit.

Higher-order time-dependent deformations of the core, related to its mass quadrupole moment, are required.

GW luminosity from spheroidal CC in the weak gravity limit

We provide a first estimate of the GW luminosity from CC, **assuming that the core has a spheroidal geometry** with time-varying axes length $a(t)$ and $c(t)$:

$$\frac{x^2}{a^2(t)} + \frac{y^2}{a^2(t)} + \frac{z^2}{c^2(t)} = 0 \quad (47)$$

If the core has a non-negligible angular momentum J (along axis z), even starting from an almost spherical configuration at large radius, one can induce ellipticity through centrifugal acceleration during collapse (if J is conserved). Angular momentum provides centrifugal support for a , while the polar axis c collapses.

A homogeneous spheroidal core has non-vanishing components of the quadrupole moment:

$$I_{xx} = I_{yy} = \rho_c \int x^2 dV = (M_{core}/15)(c^2 - a^2) \quad I_{zz} = \rho_c \int z^2 dV = (2M_{core}/15)(a^2 - c^2) \quad (48)$$

The **reduced quadrupole moment** ($I_{ij} - (1/3)\delta_{ij}I$) for such a configuration is then:

$$\tilde{I}_{ij} = \begin{pmatrix} (M_{core}/15)(c^2 - a^2) & 0 & 0 \\ 0 & (M_{core}/15)(c^2 - a^2) & 0 \\ 0 & 0 & (2M_{core}/15)(a^2 - c^2) \end{pmatrix}$$

From eq. (39), the GW luminosity is then:

$$\begin{aligned} L^{GW} &= \frac{1}{5} \frac{G}{c^5} \left\langle \frac{d^3 \tilde{I}_{ij}}{dt^3} \frac{d^3 \tilde{I}_{ij}}{dt^3} \right\rangle = \frac{1}{5} \frac{G}{c^5} \left\langle \left(\frac{d^3 \tilde{I}_{11}}{dt^3} \right)^2 + \left(\frac{d^3 \tilde{I}_{22}}{dt^3} \right)^2 + \left(\frac{d^3 \tilde{I}_{33}}{dt^3} \right)^2 \right\rangle \\ &= \frac{1}{5} \frac{G}{c^5} \frac{M_{core}^2}{15^2} \left\langle (a^{2'''} - c^{2'''})^2 + (a^{2'''} - c^{2'''})^2 + 4(a^{2'''} - c^{2'''})^2 \right\rangle \\ &= \frac{2}{375} \frac{G M_{core}^2}{c^5} \left\langle (a^{2'''} - c^{2'''})^2 \right\rangle \quad \begin{aligned} a^{2'''} &= d^3 a^2 / dt^3 \\ c^{2'''} &= d^3 c^2 / dt^3 \end{aligned} \quad (49) \end{aligned}$$

Emission of GWs depends on the relative rate of change of the two axes.

For small core angular momentum, J can be approximated with the following expression (Maclaurin spheroid):

$$J = (2M_{core}/5)^{3/2}(Ga)^{1/2}e \quad e \rightarrow 0 \quad (50)$$

$$e^2 = 1 - c^2/a^2 \quad \text{eccentricity} \quad (51)$$

As $a^2 - c^2 = a^2e^2 \propto J^4e^{-2}$, assuming that J is conserved, from eq. (50) we finally have (small J and e):

$$L^{GW} \propto J^4 \langle (e^{-2''})^2 \rangle \quad (52)$$

For very small J , L^{GW} goes rapidly to zero. For very large J the spheroid never collapses because of the large centrifugal acceleration. Thus, L^{GW} **goes to zero for both small and large J , reaching a maximum at some intermediate value J_{max} .**

This likely occurs when the rotational energy of the collapsing core becomes comparable to its gravitational potential energy and the core flattens (e grows) as it reaches nuclear density.

If the core bounces several times, then e can grow even further, leading to stronger and longer emission.

**Astrophysical sources of gravitational waves:
from core-collapse of massive stars to double compact object binaries**

**Core bounce, oscillations, convection and radiation-hydro instabilities:
Properties of the GW signal**

An estimate of the GW strain produced by CC can be obtained from the approximate quadrupole eq. (4):

$$h \simeq \frac{GM_{core}}{c^2 r} \frac{v^2}{c^2} = 10^{-20} (10 \text{ kpc}/r) \quad (53)$$

$$M_{core} \sim 1 M_{\odot} \quad v/c \sim 0.1 \quad (54)$$

Comparing with the sensitivity curves of advanced interferometers in Figure 4, we see that **Galactic supernovae (distance < 10 kpc) are detectable, but detection beyond 1 Mpc (Local Group) is essentially unfeasible.**

This implies that detectable events are limited by the Galactic supernova rate which is not larger than ~ 1 every 10 years.

Calculations using results of detailed multi-dimensional relativistic radiation-hydro simulations of CC and its evolution show that the typical features of GW signals are:

- **Strong peak at core bounce, usually followed by a ring down** (small amplitude oscillations).

- In a small number of cases, multiple (lower frequency) peaks when core bounces with re-expansion. Rather frequent in Newtonian calculations, almost absent in GR calculations because of the deeper potential.

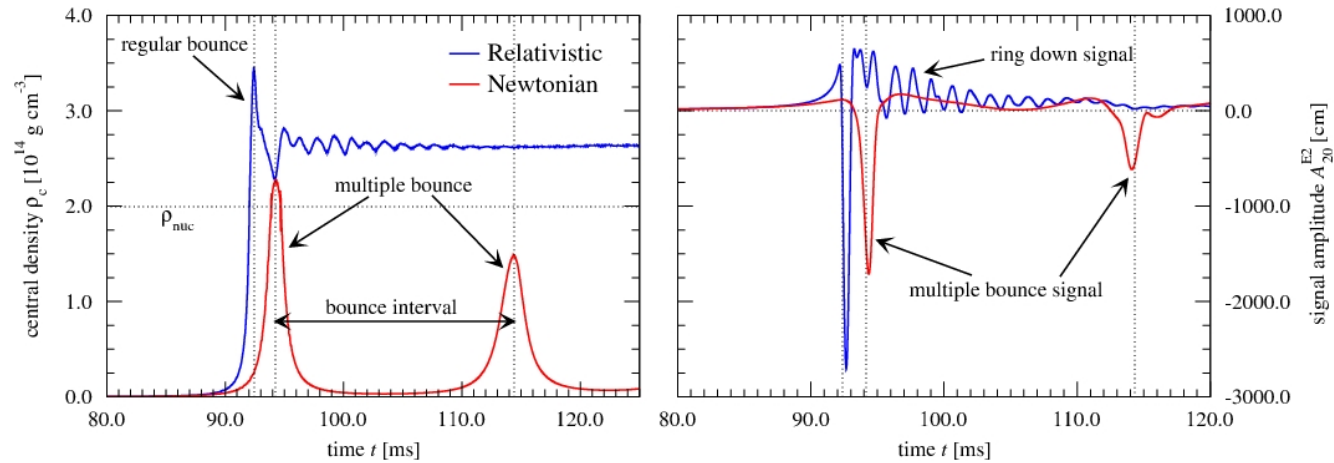


Figure 9 – Left: Core central density as a function of time. Right: GW signal measured at the outer core as a function of time (Dimmelmeier, Font & Müller 2002).

Computed GW signals can be used to tune search algorithms.

Comparison of the properties of GW signals and their features with detected signals will allow to study directly the physics of CC.

- Models with detailed microphysics and neutrino transport physics for non- or slowly rotating stars show significant non-spherical (post-bounce) flows, caused by neutrino-driven convection and radiation-hydro instabilities (e.g. SASI) below the shock. This can produce a **strong post-bounce GW signal**.

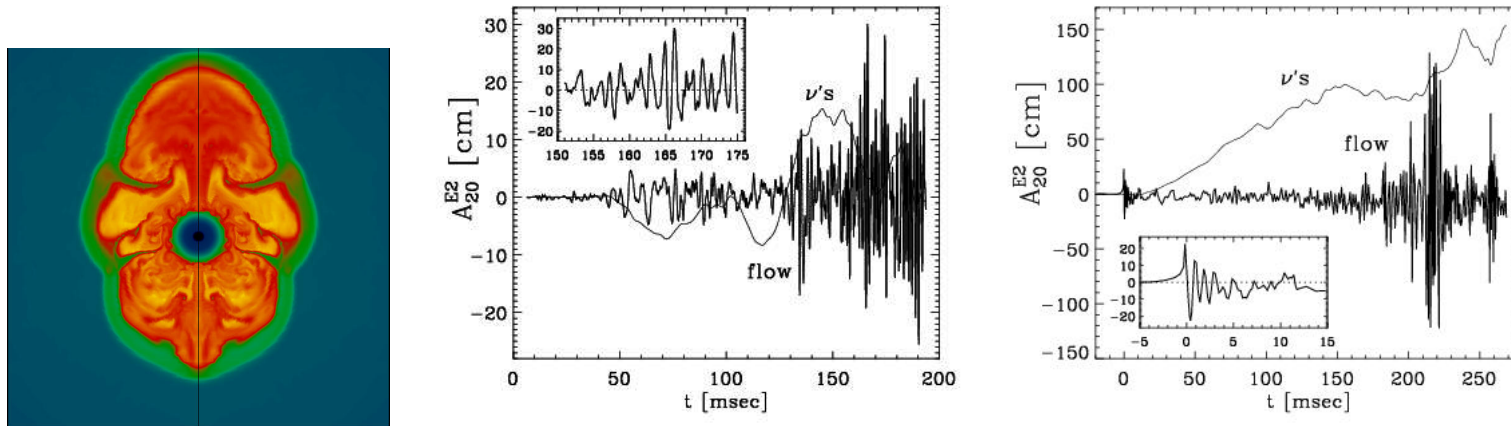


Figure 10 – Left: Snapshot of CC hydro simulation for a non-rotating $11.2 M_{\odot}$ star. Center: GW strain for CC of a non-rotating $11.2 M_{\odot}$ star. Right: GW strain for CC of a rotating $15 M_{\odot}$ star (Müller et al. 2004).

- Fourier transform of $h(t)$ provides the **frequency spectrum $h(\nu)$ of GW signals**. Characteristic frequencies are related to the dynamical timescale of the flow in the core and the neutrino-driven wind below the shock:

$$\nu_{core} = t_{dyn,core}^{-1} = v/R_{core} = 0.1c/R_{core} = 3kHz \quad (55)$$

$$\nu_{wind} = t_{dyn,wind}^{-1} = v/(10 R_{core}) = 0.01c/R_{core} = 300Hz \quad (56)$$

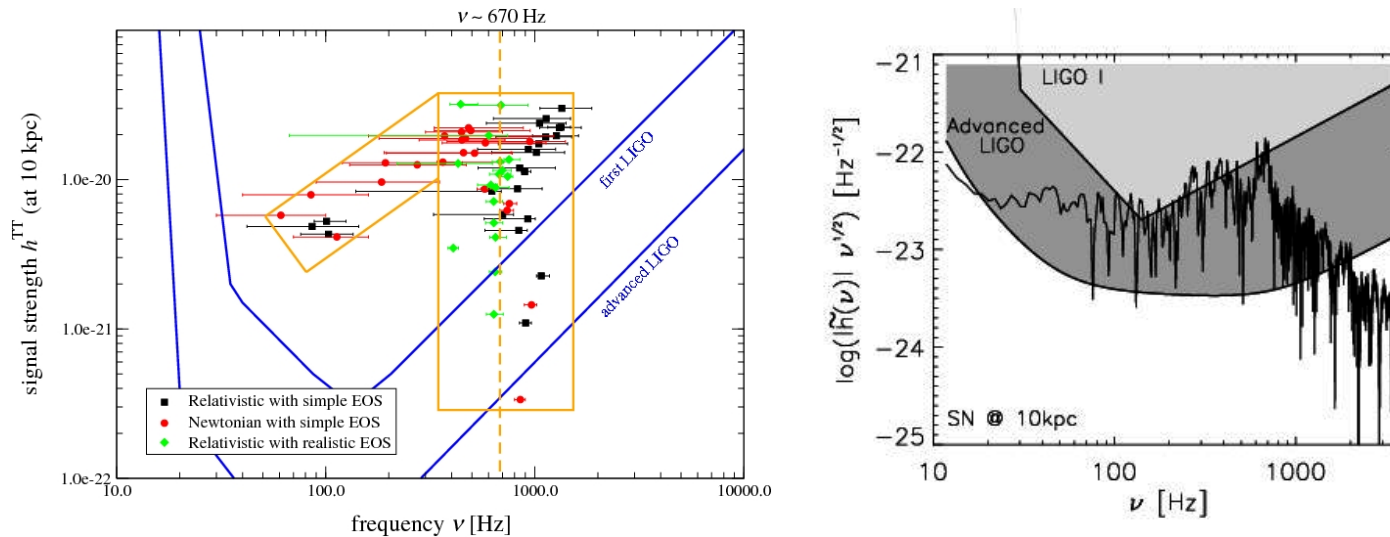


Figure 11 – Left: GW bounce signal of a Galactic CC supernova (Ott et al. 2007) at 10 kpc. Right: Post-bounce GW spectrum from CC of a rotating $15 M_{\odot}$ star at 10 kpc (Müller et al. 2004).

**Astrophysical sources of gravitational waves:
from core-collapse of massive stars to double compact object binaries**

Rotation-induced bar instability of the newborn neutron star

If the angular momentum J of the core is large, the newly born neutron star might develop triaxial instabilities caused by the backreaction of the GW metric deformations onto the neutron star itself (GR is highly non-linear in the strong gravity limit).

Such instabilities (bar instability, secular instability) can lead to non-negligible quadrupole moments and become themselves sources of GWs. Waveforms can reveal information on EOS of nuclear matter. They can only be studied with 3D radiatio-hydro simulations.

If the pre-collapse core has very high angular momentum, the collapse may produce a flattened, centrifugally supported disc. To shrink down, the disc must shed most of its angular momentum and may do it in hydrodynamics waves and/or GWs. It is unknown how many stars may follow this channel.

It has been proposed also that accretion from the pre-supernova inner mantle may increase angular momentum and trigger instabilities.

**Astrophysical sources of gravitational waves:
from core-collapse of massive stars to double compact object binaries**

4. DOUBLE PULSARS AND GRAVITATIONAL RADIATION
FROM INSPIRAL AND MERGER OF DOUBLE COMPACT OBJECT BINARIES

- (a) **Radio pulsars, Double pulsars, Binaries with Neutron Stars and Black Holes**
- (b) **GWs from a Newtonian binary: orbital period decay, inspiral waveforms, direct GW detection**
- (c) **Accurate waveforms: Measuring coalescing binary GW signals and extracting physical information**
- (d) **Mapping spacetime (bothrodesy) and GWs as standard candles/sirens for Cosmology**

**Astrophysical sources of gravitational waves:
from core-collapse of massive stars to double compact object binaries**

Radio pulsars, Double pulsars, Binaries with Neutron Stars and Black Holes

We have seen that core collapse of a massive ($M_* > 8 M_\odot$) star leads to a supernova explosion and the formation of a hot ($10^{10} K$) and dense ($10^{14} g/cm^3$) core, that cools by neutrino diffusion and convection.

In a few tens of seconds the (proto-neutron-star) core becomes a neutron-star (NS):

$$M_{NS} \simeq 1.5 M_\odot \quad R_{NS} \simeq 20 \text{ km} \quad P_{NS} \simeq 1 \text{ ms} \quad B_{NS} \simeq 10^{13} \text{ Gauss} \quad (57)$$

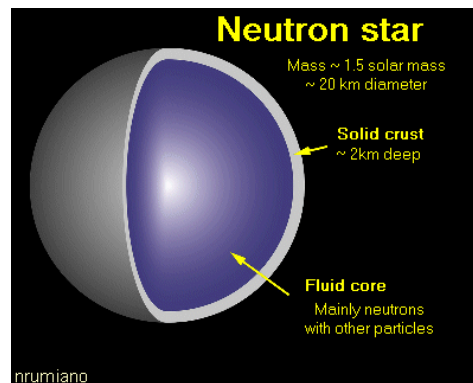


Figure 12 – A schematic representation of a Neutron Star (NS).

The **discovery of radio pulsars** in 1967 by Jocelyn Bell e Antony Hewish (Nobel in 1974) confirmed the existence of NSs. The association of many of them to supernova remnants confirmed also that they are produced in supernova explosions.

- **Radio pulsars emit periodic pulses in the radio band**, produced by a beam of radiation in the magnetosphere that points in our direction at each rotation, in what is usually referred to as the lighthouse effect.
- Such a **rotating magnetic dipole**, with the magnetic field misaligned with respect to the rotation axis, is losing energy at the expense of its rotational energy and hence is decelerating in time.
- *The properties of the rotating magnetic dipole required to account for the observed rotational period and period evolution are only consistent with the existence of a NS.*

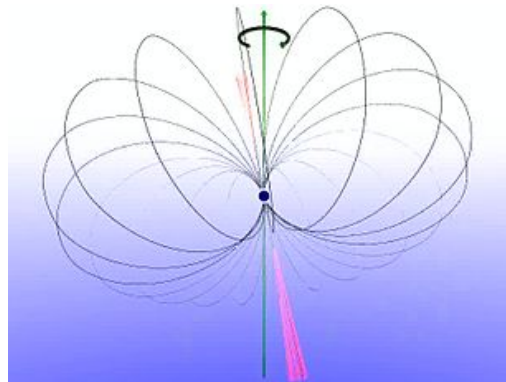


Figure 13 – Radio pulsar as a rotating magnetic dipole (cr.: Jm Smits).

Double radio pulsars

These are **binary systems consisting of 2 radio pulsars**, both favourably oriented to be seen from Earth.

One of these systems, **PSR J0737-3039** (Burgay et al. 2003, Lyne et al. 2004), stands out for its unique properties (*inferred from a detailed relativistic analysis of the arrival times of the pulses*):

- Two active radio pulsars:
Pulsar A: $P = 22.7 \text{ ms}$, $\dot{P} = 1.8 \times 10^{-18} \text{ s/s}$
Pulsar B: $P = 2.77 \text{ s}$, $\dot{P} = 9 \times 10^{-16} \text{ s/s}$
- Very accurately measured (gravitational) masses, characteristic age ($\tau = P/2\dot{P}$) and surface magnetic field ($B = 3.2 \times 10^{19} \sqrt{P\dot{P}} \text{ Gauss}$):
 $M_A = (1.3381 \pm 0.0007) M_{\odot}$, $\tau_A = 210 \text{ Myr}$, $B_A = 6.3 \times 10^9 \text{ Gauss}$
 $M_B = (1.2489 \pm 0.0007) M_{\odot}$, $\tau_B = 50 \text{ Myr}$, $B_B = 1.2 \times 10^{12} \text{ Gauss}$
- A very short orbital period of 2.4 hours, an average orbital separation of $\sim 1.25 R_{\odot}$ and a small eccentricity of 0.088
- Regular eclipses and clear evidence of strong interactions between the two magnetospheres.

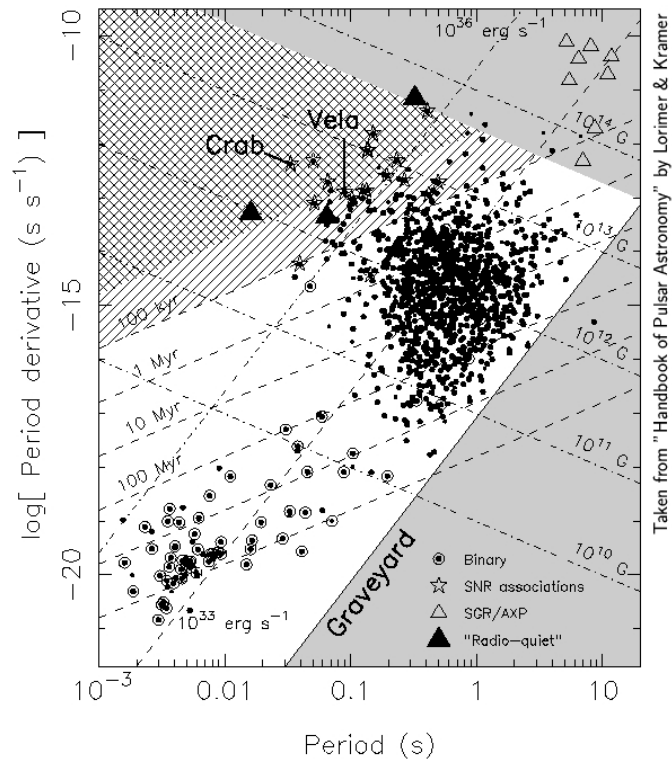


Figure 14 – $P - \dot{P}$ diagram for the known pulsar population.

This amazing system provides the best test, at present, of GR in relatively strong gravity.

- In Newtonian gravity, the two stellar masses of the binary are unknown parameters. If measurable, GR effects (among which the orbital period decay,

periastron advance, gravitational redshift and second-order Doppler shift) provide additional relations among the keplerian and additional post-Keplerian (PK) parameters.

- For PSR J0737-3037A/B, 5 PK parameters are precisely measured, plus the projected semi-major axis of the second pulsar. Thus, [the system allows us to measure both pulsar masses and provides \$5+1-2=4\$ timing tests of GR. The additional 4 measured and computed PK parameters agree to better than 0.1%.](#)
- Other relativistic effects (e.g. spin-orbit coupling, aberration and gravitational lensing) may be measurable in the near future, providing further constraints and measurements (e.g. the NS moment of inertia).

Black Hole (BH) formation and NS-BH, BH-BH binaries

While NS-NS binaries are observed as radio pulsars, *we do not have any direct evidence, to date, of the existence of BH-NS and BH-BH binaries.* However, we do observe BHs in binary systems accreting from ordinary stars (X-ray binaries).

[We have a convincing theoretical understanding of the formation of stellar-mass BHs.](#) They form in the aftermath of a supernova explosion (as NSs).

- During the passage of the shock through the envelope of the star, the energy deposited by the shock wave in the inner shells is lost in accelerating the layers on the top, so that ejecta velocity increases outwards (homologous expansion).

- If the envelope of the pre-supernova star is sufficiently massive ($\sim 25 - 40 M_{\odot}$), after explosion the inner low-velocity ejecta (below the He layer) may remain gravitationally bound and **fall-back** onto the NS on a dynamical time (hours).
- If the fallback mass is sufficiently large (from a few tenths to a few M_{\odot}), the mass deposited onto the NS overcome the maximum mass allowed by the EOS of nuclear matter ($M_{NS,max} \sim 2 - 3 M_{\odot}$) and **the NS itself may collapse into a BH**.

Heavier stellar BHs (with masses up to $M_{NS,max} \sim 80 M_{\odot}$) can form from direct collapse (without supernova explosion and NS formation) of heavier stars (with pre-supernova masses $> 40 M_{\odot}$). This requires low metallicity ($Z \sim 0.1 - 0.01 Z_{\odot}$), to reduce the efficiency of wind mass-loss during the star's life.

To form NS-NS, BH-NS, BH-BH binaries then requires suitable paths in the evolution of binary systems with massive stars, studied with population-synthesis codes for systems in isolation and with codes dealing with dynamical interactions for systems in stellar clusters (see M. Mapelli's lecture).

These calculations include stellar evolution effects and the effects of the significant NS recoil that occurs at core bounce (NS kick velocity). Merger rates are theoretically computed in this way.

**Astrophysical sources of gravitational waves:
from core-collapse of massive stars to double compact object binaries**

**GWs from a Newtonian binary:
orbital period decay, inspiral waveforms, direct GW detection**

We consider now the GW emission and evolution of a double compact object (NS-NS, NS-BH, BH-BH) binary. M_1 and M_2 are the masses of the two objects (considered point-like) and a is the radius of the (circular) orbit.

We start calculating the reduced mass quadrupole of the binary (eq. [32]). Assuming the orbit in the $z = 0$ plane and its center at the origin, the non-vanishing components of I_{ij} are:

$$\begin{aligned}
 I_{xx} &= x_1^2 M_1 c^2 + x_2^2 M_2 c^2 = (a_1^2 M_1 c^2 + a_2^2 M_2 c^2) \cos^2 \phi = \mu a^2 \cos^2 \phi \\
 I_{yy} &= y_1^2 M_1 c^2 + y_2^2 M_2 c^2 = (a_1^2 M_1 c^2 + a_2^2 M_2 c^2) \sin^2 \phi = \mu a^2 \sin^2 \phi \\
 I_{xy} &= I_{yx} = x_1 y_1 M_1 c^2 + x_2 y_2 M_2 c^2 = (a_1^2 M_1 c^2 + a_2^2 M_2 c^2) \sin \phi \cos \phi = \mu a^2 \sin \phi \cos \phi
 \end{aligned} \tag{58}$$

where

$$\begin{aligned}
 a &= a_1 + a_2 & x_{1,2} &= a_{1,2} \cos \phi & y_{1,2} &= a_{1,2} \sin \phi \\
 \mu &= M_1 M_2 / M & M &= M_1 + M_2 & \mu a &= M_1 a_1 = M_2 a_2
 \end{aligned}$$

From eqs. (58), we obtain the reduced quadrupole moment (eq. [37]):

$$\tilde{I}_{ij} = I_{ij} - \frac{1}{3}\delta_{ij}I = \begin{pmatrix} (\mu/2)a^2 \cos 2\phi + c_{xx} & (\mu/2)a^2 \sin 2\phi & 0 \\ (\mu/2)a^2 \sin 2\phi & -(\mu/2)a^2 \cos 2\phi + c_{yy} & 0 \\ 0 & 0 & 0 \end{pmatrix}$$

where c_{ii} are constants. The GW luminosity of the binary (eq. [39]) is then:

$$\begin{aligned} L^{GW} &= \frac{1}{5} \frac{G}{c^5} \left\langle \frac{d^3 \tilde{I}_{ij}}{dt^3} \frac{d^3 \tilde{I}_{ij}}{dt^3} \right\rangle = \frac{1}{5} \frac{G}{c^5} \left\langle \left(\frac{d^3 \tilde{I}_{xx}}{dt^3} \right)^2 + \left(\frac{d^3 \tilde{I}_{yy}}{dt^3} \right)^2 + 2 \left(\frac{d^3 \tilde{I}_{xy}}{dt^3} \right)^2 \right\rangle \\ &= \frac{1}{5} \frac{G}{c^5} \left(\frac{\mu a^2}{2} \right)^2 (2\Omega)^6 \langle 2 \sin^2 2\phi + 2 \cos^2 2\phi \rangle = \frac{32 G^4 M^3 \mu^2}{5 c^5 a^5} \end{aligned} \quad (59)$$

where $\phi = \int \Omega dt$ and $\Omega^2 = GM/a^3$ (III Kepler law).

The GW luminosity is emitted at the expense of the orbital energy. We can then compute the orbital decay ($\tilde{M} = M^{2/5} \mu^{3/5}$ is called **chirp mass**):

$$E_{orb} = \frac{1}{2} M_1 a_1 \Omega^2 + \frac{1}{2} M_2 a_2 \Omega^2 - G \frac{M_1 M_2}{a} = -\frac{G \mu M}{2a} \quad (60)$$

$$\frac{dE_{orb}}{dt} = -L^{GW} \quad \frac{dE_{orb}}{da} \frac{da}{dt} = -L^{GW} \quad a \rightarrow 0 \text{ for } t \rightarrow t_c \quad (61)$$

$$a(t) = \left[\frac{256 G^3 M^2 \mu}{5 c^5} (t_c - t) \right]^{1/4} \quad \Omega(t) = \left[\frac{256 G \tilde{M}^{5/3}}{5 c^5} (t_c - t) \right]^{-3/8} \quad (62)$$

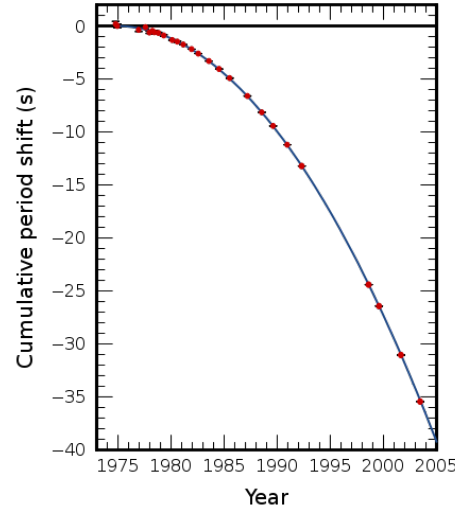


Figure 15 – Orbital period decay $P(t) - P(t_0) = 2\pi(1/\Omega(t) - 1/\Omega(t_0))$ of the NS binary pulsar PSR B1913+16 (discovered by Hulse & Taylor in 1974, for which they won the 1993 Nobel Prize in Physics).

Finally, from eq. (33) and (58), we derive the dependence of the waveforms on time:

$$\begin{aligned}\bar{h}_{xx} &= \frac{2G}{rc^4} \frac{d^2}{dt^2} I_{xx} = -\frac{4G^2 M \mu}{rc^4} \frac{1}{a} \cos 2\phi = -\frac{4G^2 \tilde{M}}{rc^4} \left(\frac{G\tilde{M}}{c^3} \Omega \right)^{2/3} \cos 2\phi \\ \bar{h}_{yy} &= \frac{2G}{rc^4} \frac{d^2}{dt^2} I_{yy} = \frac{4G^2 M \mu}{rc^4} \frac{1}{a} \cos 2\phi = \frac{4G^2 \tilde{M}}{rc^4} \left(\frac{G\tilde{M}}{c^3} \Omega \right)^{2/3} \cos 2\phi \\ \bar{h}_{xy} &= \bar{h}_{yx} = \frac{2G}{rc^4} \frac{d^2}{dt^2} I_{xy} = -\frac{4G^2 M \mu}{rc^4} \frac{1}{a} \sin 2\phi = \frac{4G^2 \tilde{M}}{rc^4} \left(\frac{G\tilde{M}}{c^3} \Omega \right)^{2/3} \sin 2\phi\end{aligned}\quad (63)$$

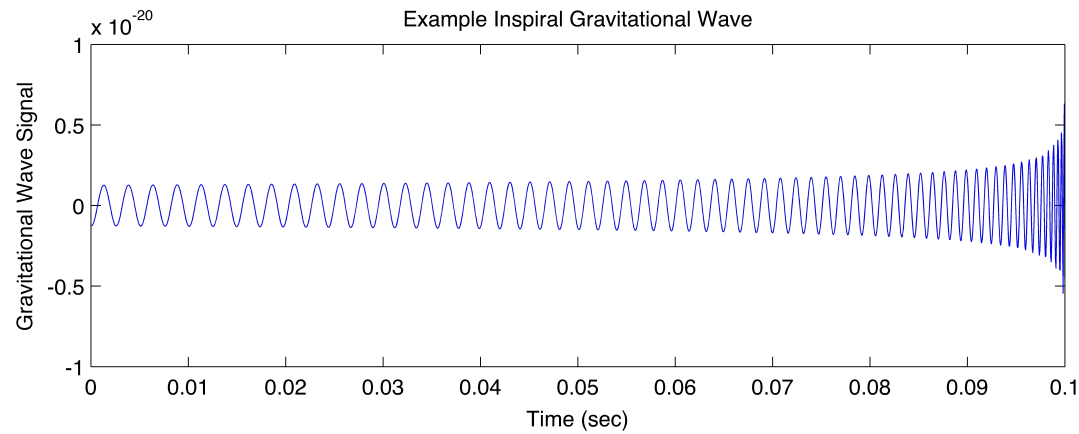


Figure 16 – [Waveform of a Newtonian binary.](#)

For PSR J0737-3039, the orbital frequency is $\Omega = 1.16 \times 10^{-4}$ Hz. The expected strain is $h \sim 5 \times 10^{-21}$ at $2\Omega = 2.3 \times 10^{-4}$ Hz. **This is above the 1-year sensitivity for the future space interferometer** (Laser Interferometric Space Antenna). GW detection will provide a test to GR and an independent distance measurement.

**Astrophysical sources of gravitational waves:
from core-collapse of massive stars to double compact object binaries**

**Accurate waveforms: Measuring coalescing binary GW signals
and extracting physical information**

A system like PSR B1913+16 will merge in about 300 Myr (from eq. [62]). PSR J0737-3039 will do it in 85 Myr.

When this will happen, in 15 minutes GWs will sweep up in frequency from 10 Hz to 1000 Hz. **It is this last 15 minutes of inspiral, with ~ 16000 cycles, and the final coalescence and ring down that LIGO/VIRGO seeks to discover.**

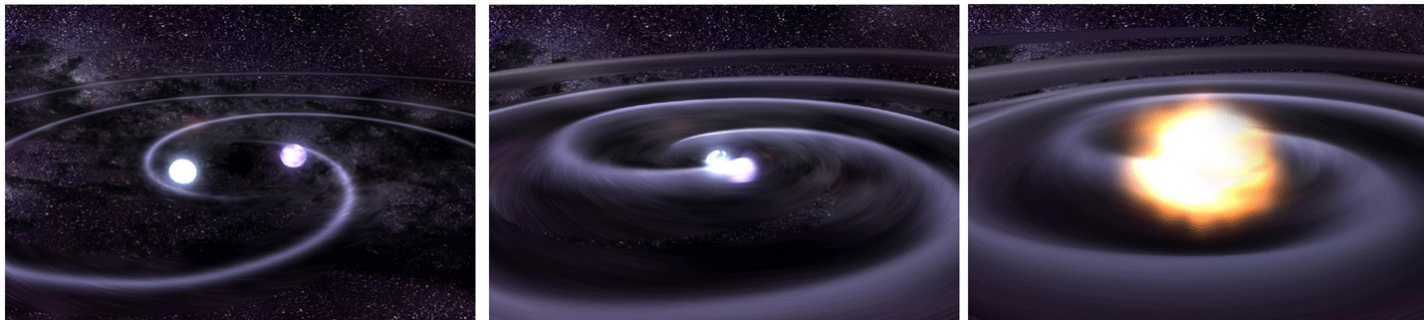


Figure 17 – Artist's impression of a binary merger (Cr.: NASA/CXC/GSFC/T.Strohmayer).

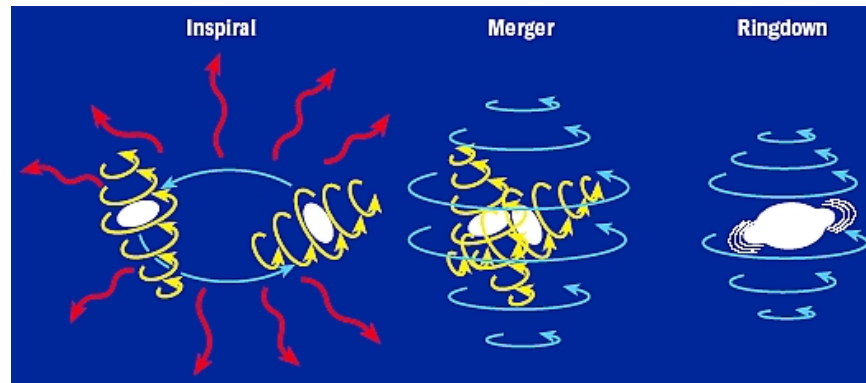


Figure 18 – Schematic illustration of the three stages of a compact binary merger.

Inspiral waveforms

- A GW interferometer measures a superposition of the two polarization states $+$ and $-$ (eq. [2]). The coefficients depend on the position of the source on the sky (2 angles).
- Eq. (62) shows that, in the Newtonian approximation, the GW pulsation and its rate of variation $d\Omega/dt$ (*chirp*) is determined solely by the so called chirp mass $\tilde{M} = M^{2/5}\mu^{3/5}$.
- Eq. (63) shows that the GW waveform amplitudes depend on the chirp mass \tilde{M} , the distance to the source r and the pulsation Ω (or frequency $f = \Omega/2\pi$).

- It is not difficult to show also that the ratio of the amplitudes of the two polarization states $+$ and $-$ depends on the inclination angle i of the orbit:

$$|h_x^{TT}|/|h_+^{TT}| = 2 \cos i / (1 + \cos^2 i) \quad (64)$$

- Less easy is to see that, if the orbit is not circular but has a certain eccentricity e , the waveform shape and hence its harmonic content depend on e .

Thus, by measuring the two polarization amplitudes, the pulsation (or frequency) and its chirp, and the harmonic content of the inspiral GW signal, one can determine directly the physical quantities r , \tilde{M} , i , e .

To determine the direction of the source on the sky, one needs to compare the polarization amplitudes measured by more detectors in different positions.

Calculations of GR waveforms (with higher order mass moments) reveal that *non-linear gravity effects* (e.g. *GW backscattering onto spacetime curvature, relativistic precession*) provide additional information, influencing the chirp and producing modulations dependent on the ratio μ/M (and on spins and orbital angular momentum).

Coalescence and ring down waveforms

For an accurate description of this phase, numerical relativity and high order post-Newtonian calculations are required.

- **NS-NS coalescence:** GWs are **sensitive to EOS of nuclear matter**. Observing NS-NS coalescence would allow us to study the nuclear matter EOS, but also relativistic collisions of very high nucleon-numbers nuclei.

Unfortunately, the final phase of the coalescence is mostly out of the sensitivity window of ground based interferometers ($f > 1$ kHz).

- **NS-BH coalescence:** If the BH has a mass $> 10M_{\odot}$, the NS should be swallowed as a whole. If it is less massive and/or rapidly rotating, then the NS will be tidally disrupted before being swallowed. As with NS-NS coalescence, **waveforms will carry information on the EOS of nuclear matter** and will be in the kHz range.

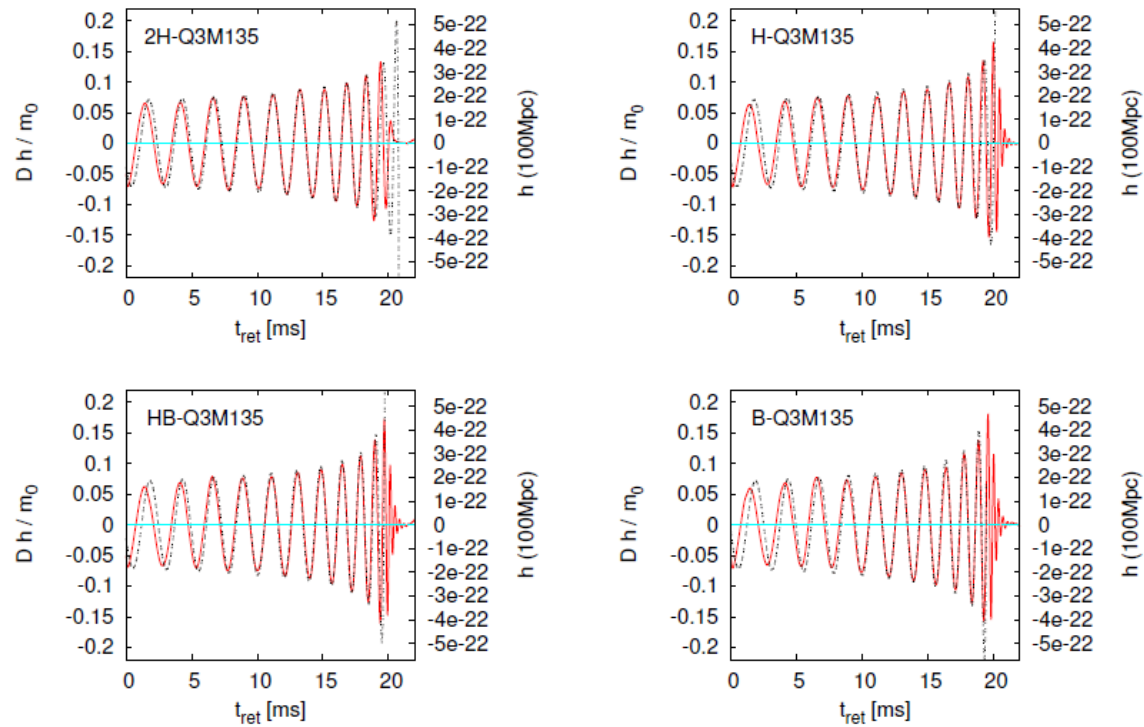


Figure 19 – Gravitational waveforms for NS-BH coalescence observed along the axis perpendicular to the orbital plane for very stiff (2H), stiff (H), moderate (HB), and soft (B) EOS (Kyutoku et al. 2010, Phys. Rev. D, 82, 044049; Shibata & Taniguchi, 2011, Living Rev. Relativity 14, 6).

- **BH-BH coalescence:** It will excite **large-amplitude highly non-linear vibrations of space-time near to BH horizon**. Especially interesting will be the

case of two spinning BHs with axes misaligned with each other and with the orbital angular momentum, because of relativistic precession.

Computing waveforms requires powerful supercomputer simulations.

GWs will allow us to map the mass and spin distributions of coalescing binaries.

Measuring GW binary signals

The weakness of the signal requires a careful tracking of its phase and frequency.

The procedure is similar to that adopted for radio pulsars, for which a phenomenological model for the phase and/or frequency evolution is fitted or cross-correlated with the data.

The fit is minimized or the cross-correlation is maximized when the parameters of the model accurately describe the signal. For a signal N_c cycles long, the cross-correlation is enhanced by roughly $\sqrt{N_c}$.

Similarly, for a binary GW signal, one cross-correlates model waveforms against data, looking for a model and corresponding parameters that maximize the correlation.

The need to produce detailed model of the waveforms to this purpose has been a major motivation for the development of perturbation theory, post-Newtonian theory and numerical relativity.

**Astrophysical sources of gravitational waves:
from core-collapse of massive stars to double compact object binaries**

**Mapping spacetime (bothrodesy)
and GWs as standard candles/sirens for Cosmology**

- Earth's gravity is mapped with the motion of satellites (geodesy). One can imagine to do the same for **extreme mass ratio binaries**, for which the orbits of the smaller component can be used to map the space-time of the bigger compact object (bothrodesy, from $\beta\theta\rho\zeta$ which in Greek means sacrificial pit).

Matching the signal with templates produced by different time-varying mass moments (and mass currents), one can map the space-time and probe, e.g., the Schwarzschild or Kerr solutions for BHs. *Mass and spin can be determined with an accuracy of 0.1% or better.*

- **Binary inspiral are standard candles.** In fact, standard sirens because they provide a 'stereophonic' view, not an image, of a source. **Detecting GWs from merging binaries at Cosmological distances provides a measurement of the luminosity distance. All the other parameters (including the masses) are determined modulo a factor $(1 + z)$.**

Thus, if it possible to measure the source's redshift independently (e.g. from EWs), then it may be possible to place constraints on Cosmological models, with completel different systematic properties than other standard candles.

**Astrophysical sources of gravitational waves:
from core-collapse of massive stars to double compact object binaries**

REFERENCES

1. Dimmelmeier, H. et al., *Relativistic simulations of rotational core collapse. I. Methods, initial models, and code tests*, A&A, 2002, 388, 917
2. Dimmelmeier, H. et al., *Relativistic simulations of rotational core collapse. II. Collapse dynamics and gravitational radiation*, A&A, 2002, 393, 523
3. Hughes, S.A., *Gravitational waves from merging compact binaries*, 2009, ARA&A, 47, 107
4. Kramer, M. & Stairs, I.H., *The double pulsar*, 2008, ARA&A, 46, 541
5. Müller, E. et al. 2004, *Towards gravitational wave signals from realistic core collapse supernova models*, ApJ, 603, 221
6. Shapiro, S. L. & Teukolsky, S. A., *Black holes, white dwarfs, and neutron stars: The Physics of compact objects*, 2002, chapter 16
7. Thorne, K., *Probing black holes and other exotic objects with gravitational waves*, 1998, in Proceedings of the conferences “Relativistic Astrophysics”, Eds. B.J.T. Jones & D. Marković, p. 259